Heterogeneous Catalysis

DOI: 10.1002/anie.200905815

Subsurface-Controlled CO_2 Selectivity of PdZn Near-Surface Alloys in H_2 Generation by Methanol Steam Reforming**

*Christoph Rameshan, Werner Stadlmayr, Christian Weilach, Simon Penner, Harald Lorenz, Michael Hävecker, Raoul Blume, Tulio Rocha, Detre Teschner, Axel Knop-Gericke, Robert Schlögl, Norbert Memmel, Dmitry Zemlyanov, Günther Rupprechter, and Bernhard Klötzer**

For the use of polymer electrolyte membrane fuel cells (PEMFC) in electric power generation, an efficient source of clean hydrogen is needed. To avoid technical and safety problems of hydrogen handling, storage, and transport, methanol can be used as practical and abundant energy carrier for stationary or on-board H_2 generation, and it also has the advantage of a high energy density. Hydrogen generation from methanol can be performed by catalytic methanol steam reforming (MSR) [Eq. (1)].

$$CH_3OH + H_2O \rightarrow CO_2 + 3\,H_2 \qquad (1)$$

This reaction must be carried out with high selectivity, avoiding the undesired by-product carbon monoxide, which poisons the fuel-cell electro-catalyst. A number of selective MSR catalysts are available. Apart from advanced copper-based catalysts, reduced states of Pd/ZnO, Pd/Ga_2O_3, or Pd/In_2O_3 have been identified as promising candidates.[1] Active phases in these catalysts are, however, alloys/intermetallics of PdZn, PdGa, and PdIn, that result from partial reduction of the oxide support and subsequent alloying of Pd during reductive catalyst activation (on inert supports, pure Pd produces only CO and H_2). In particular, the PdZn/ZnO catalyst combines the advantages of excellent catalytic selectivity and thermal stability.[2] However, the selectivity strongly depends on the exact experimental parameters of catalyst synthesis, oxidative and reductive gas treatments, annealing, and reaction conditions. These variables make establishing structure–selectivity correlations on industrial catalysts very difficult and it is often unknown why two marginally different treatments of the same catalyst lead to very different selectivities.

Using catalytically active model systems, in this case ultrahigh-vacuum (UHV) prepared PdZn surface alloys, combined with a detailed spectroscopic analysis of alloy structure, composition, and catalytic activity, we show that the CO_2 selectivity of a PdZn 1:1 surface alloy is governed by the subsurface layers. Whereas a "multilayer" (ca. five layers) PdZn 1:1 near-surface alloy exhibits high CO_2 selectivity, a predominantly palladium-coordinated "monolayer" PdZn 1:1 surface only produces CO and H_2, despite its identical surface composition. This situation is explained by differences in the electronic and geometric structure of the two alloy surfaces, as monitored by synchrotron-based in-situ ambient pressure X-ray photoemission spectroscopy (AP-XPS), low-energy ion scattering (LEIS), Auger electron spectroscopy (AES), polarization-modulated infrared reflection absorption spectroscopy (PM-IRAS), and kinetic tests in an all-glass reaction cell capable of operating between 10^{-10} and 1000 mbar. The results demonstrate the pronounced influence of the subsurface composition on the electronic and the geometric structures of the surface layer, which in turn govern the unique bifunctional catalytic action of the PdZn multilayer alloy: the predominant transformation of methanol to formaldehyde and the activation of water as ZnOH species.

PdZn (near-)surface alloys grown by Zn deposition in ultrahigh vacuum on a Pd(111) single crystal have been examined by a number of groups in recent years.[3–7] Based on these studies, a procedure was developed to prepare defined PdZn 1:1 alloy surfaces on Pd substrates, which are only different with respect to their Pd:Zn subsurface composition. For simplicity we denoted them as "multilayer" and "monolayer" alloy states. Both have a p(2×1) structure with a 1:1 PdZn surface ratio on Pd(111), as verified by low-energy electron diffraction (LEED; see Supporting Information, Scheme S5).

[*] W. Stadlmayr, Dr. S. Penner, H. Lorenz, Prof. N. Memmel, Dr. B. Klötzer
Institute of Physical Chemistry, University of Innsbruck
Innrain 52 A, 6020 Innsbruck (Austria)
Fax: (+43) 512-507-2925
E-mail: Bernhard.Kloetzer@uibk.ac.at
Homepage: http://www.uibk.ac.at/physchem/
C. Weilach, Prof. G. Rupprechter
Institute of Materials Chemistry, Vienna University of Technology
Veterinärplatz 1, 1210 Vienna (Austria)
Dr. D. Zemlyanov
Birck Nanotechnology Center, Purdue University
1205 West State Street, West Lafayette, IN 47907-2057 (USA)
C. Rameshan, Dr. M. Hävecker, Dr. R. Blume, Dr. T. Rocha, Dr. D. Teschner, Dr. A. Knop-Gericke, Prof. R. Schlögl
Department of Inorganic Chemistry, Fritz-Haber-Institute of the Max-Planck-Society
Faradayweg 4–6, 14195 Berlin (Germany)

[**] This work was financially supported by the Austrian Science Fund through grant P208920-N19 and the TU Vienna (IP-VSFG). C.R. acknowledges a PhD scholarship granted by the Max Planck Society. Support for the measurements at HZB/BESSY II was granted through EU program RII3-CT-2004-506008, proposal No. 2008_2_80336. The authors thank the HZB/BESSY II staff for their support of the in situ X-ray photoemission spectroscopy.

Supporting information for this article is available on the WWW under http://dx.doi.org/10.1002/anie.200905815.

The multilayer PdZn 1:1 surface alloy was prepared by evaporating 2or more monolayers (ML) of Zn onto Pd(111) or Pd foil at 300 K or below, and subsequent thermal annealing in vacuum at approximately 500 K for 10 min. The LEIS data in Figure 1a indicate an invariant PdZn 1:1 surface composition for annealing temperatures between approximately 430 and 570 K. This stability window is also corroborated by the AES data of Zn on Pd foil in Figure 1a. XPS depth profiling (varying the kinetic energy of the photoelectrons between 100 eV and 900 eV; see Supporting Information, Scheme S1) revealed that the multilayer alloy state exhibits a constant Pd/Zn composition for depths down to approximately five alloy layers.

The monolayer PdZn 1:1 surface alloy was also obtained by Zn deposition, but subsequent thermal annealing was in UHV at approximately 630 K for 10 min. Whereas the surface composition remains close to 1:1, as evident from LEIS, AES indicates that the Zn concentration in subsurface layers is considerably decreased (Figure 1a). The data depicted in Figure 1a were obtained for Zn deposited on Pd foil. Except for a small temperature shift of the multilayer stability regime by about 20 K the data correspond quite closely to that from LEIS experiments on Zn films on single-crystal Pd(111) (Figure 1b). Clearly both types of Pd substrate behave very similarly with respect to thermally induced changes of the (sub)surface composition, as we could additionally corroborate by comparing the Pd 3d core-level and valence-band XPS spectra of Pd(111) and Pd foil during thermal annealing of multilayers of Zn in ultrahigh vacuum (see Supporting Information, Figure S2). The characteristic spectral changes from a zinc-rich to a zinc-lean chemical environment of palladium (compare 500 K "multilayer" and 630 K "monolayer" spectra in Supporting Information, Figure S2) were little different, that is, at the same annealing temperature basically the same spectra were obtained for both substrates.

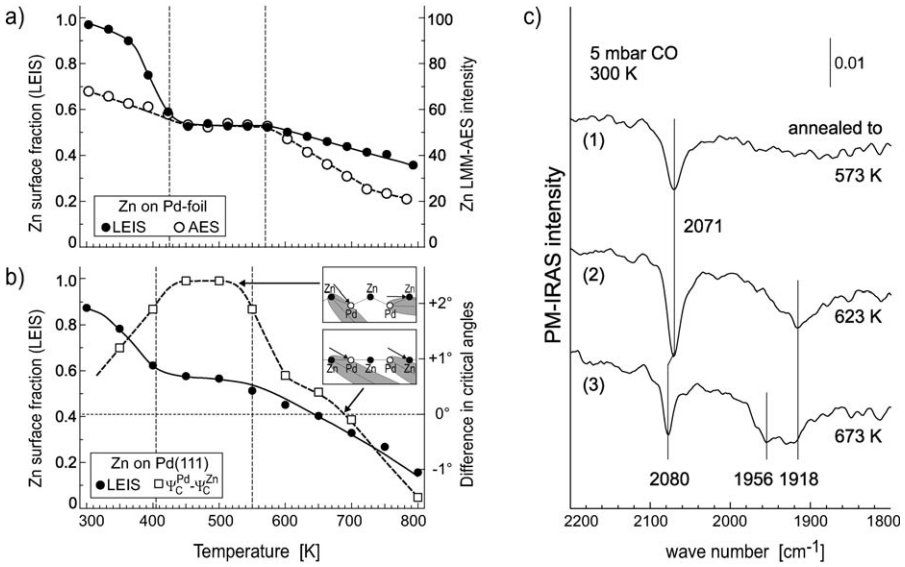

Figure 1. a) Zn surface fractions derived from LEIS (●) and peak-to-peak intensity of the differentiated Zn-$L_3M_{45}M_{45}$ (1G) Auger peak (○) as a function of annealing temperature. Initially, 3 ML of Zn were deposited at 300 K on a Pd foil. b) ●: Pd:Zn surface fractions derived from LEIS for Zn films deposited on single crystal Pd(111) (Adapted from Ref. [7]). □: Difference in critical angles for backscattering of 5 keV Ne ions from Pd and Zn atoms, respectively. Inset: schematic side views of a corrugated and a non-corrugated (2×1) PdZn surface. Arrows and gray shadow cones indicate the critical angles where backscattering from Pd and Zn atoms, respectively, sets in. For clarity the corrugation is greatly exaggerated. c) 1) PM-IRAS spectroscopy of CO adsorbed at 5 mbar and 300 K on the 1:1 PdZn multilayer alloy. Traces (2) and (3) are taken after annealing to 623 and 673 K, respectively.

The altered subsurface composition induces an altered atomic geometry (corrugation) of the surface layer as revealed by impact-collision ion scattering spectroscopy (ICISS). As shown in Figure 1b, for the 500 K multilayer state the critical angle Ψ_C^{Zn} for backscattering from Zn is approximately 2.5° lower than Ψ_C^{Pd} for Pd atoms (details of scattering geometry and definition of ψ_C are given in the Supporting Information, experimental section). This result indicates a corrugated surface with Zn atoms residing approximately 0.25 Å above their Pd counterparts.[7] In contrast, after annealing to 630 K or above, the difference in critical angles is close to zero or negative, implying that the surface corrugation vanishes or even becomes inverted. This finding is in full agreement with density functional theory (DFT) calculations for Zn films on Pd(111), which predict a "Zn-up/Pd-down" structure for 2 ML films, but "Zn-down/Pd-up" for 1 ML thick alloy films.[5]

The homogeneity of the 1:1 PdZn surface layer was examined by PM-IRAS spectroscopy using CO as probe molecule. Figure 1c, trace (1) shows a spectrum recorded under 5 mbar CO at 300 K, exhibiting a single sharp peak at 2070 cm^{-1}, characteristic of terminal CO adsorbed on top of individual Pd atoms. This feature demonstrates the structural homogeneity of the multilayer alloy surface, because any of remaining Pd islands would give rise to signals for bridging CO (at 1955 cm^{-1}) and terminal CO (at 2085 cm^{-1}) under these conditions.[8] The vibrational frequency agrees very well with that of the on-top CO peak observed for PdZn/ZnO powder catalysts.[9] The −15 cm^{-1} difference between on-top CO on Pd(111) and on PdZn is due to a DFT-predicted charge transfer from Zn to Pd,[10] enabling better back-bonding which increases the on-top CO adsorption energy but weakens the internal C–O bond, thus leading to lower wavenumbers.[11]

The lower spectra in Figure 1c show the effect of higher annealing temperatures. Owing to the lowered Zn coordination of the top layer, the 623 K monolayer zinc-lean surface alloy additionally shows a band arising from bridging CO at 1920 cm^{-1}, again in agreement with DFT calculations.[11] The intensity increase of the bands for on-top species is probably due to the changes in the surface corrugation discussed above.

Higher annealing temperatures lead to spectra with increasing contribution of CO/Pd(111) (i.e. bridge and terminal CO at 1955 cm^{-1} and 2085 cm^{-1}, respectively).

Since the multi- and monolayer alloy states only differ with respect to subsurface PdZn coordination geometry and coordination number, they represent the ideal test case for the electronic "ligand effect" influencing catalytic selectivity.

The MSR activity/selectivity of the multilayer and monolayer alloy was studied by temperature-programmed reaction in the UHV-compatible high-pressure cell operated as a recirculating batch reactor under realistic reaction conditions close to those of industrial catalysis. Figure 2 (upper panel) reveals that the multilayer PdZn 1:1 surface alloy converts CH_3OH and water into CO_2 and formaldehyde CH_2O up to a temperature of 573 K, which is the upper limit of the multilayer stability.

At temperatures above 573 K, CH_2O is consumed (negative formation rate) and converted into CO by dehydrogenation, as a result of the progressive transformation of the multilayer into the monolayer alloy at these temperatures. This result was corroborated by performing the reaction on the monolayer PdZn 1:1 surface alloy. Similar to the pure Pd substrate it exhibited no CO_2 selectivity even at reaction temperatures below 623 K (Figure 2, lower panel). Despite the virtually identical surface stoichiometry of PdZn 1:1 for both catalysts, the selectivity is markedly different. This phenomenon is consistently explained by the influence of subsurface composition on the electronic and geometric structure of the topmost "active" PdZn layer.

We note that the Zn/Pd ratios determined by intermediate- or post-reaction LEIS/AES analysis correspond to the values depicted in Figure 1 at the respective temperature, that is, the thermal change of the near-surface composition is hardly affected by the reaction mixture. Unfortunately, in-situ PM-IRAS measurements performed under reaction conditions were not sensitive enough to detect key intermediates, such as CH_2O.

The electronic differences between the multilayer and monolayer alloys are illustrated by XPS spectra acquired in situ during the reaction (Pd 3d, Zn 3d, and valence band regions, Figure 3). The Pd 3d level of the multilayer alloy exhibits its typical maximum at 335.8 eV, whereas for the monolayer surface alloy it is at 335.3 eV. The higher intensity of the monolayer Pd 3d signal and the concomitant decrease of the Zn 3d signal reflect the subsurface zinc-lean character of this surface.

The valence-band spectra reveal another significant difference. Whereas the multilayer alloy shows a "Cu-like" valence band, that is, a significantly reduced density of states between 2 eV and 0 eV, the monolayer alloy, despite its 1:1 surface composition, rather resembles a modified Pd surface

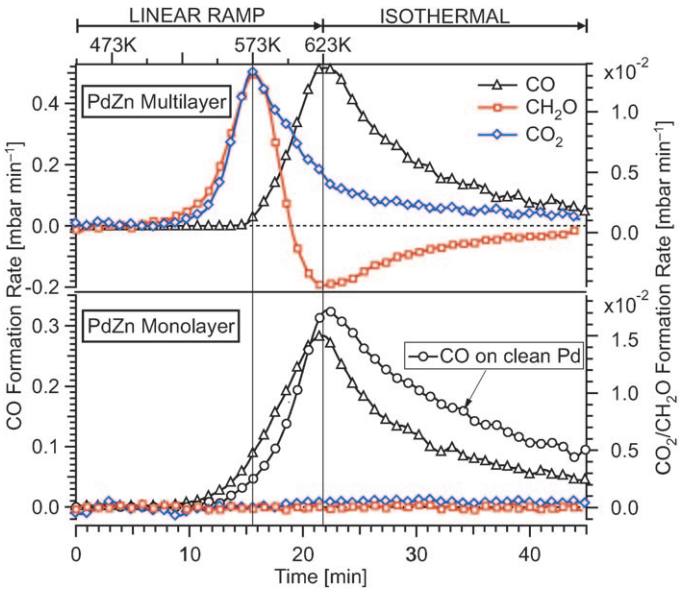

Figure 2. Temperature-programmed methanol steam reforming on the multilayer PdZn 1:1 alloy on Pd foil (upper panel) versus MSR reaction on "Zn-lean" monolayer PdZn surface and MSR reaction on clean Pd foil (lower panel). Reaction conditions: 12 mbar methanol, 24 mbar water, 977 mbar He; linear temperature ramp (9.0 K min^{-1}) up to 623 K, and subsequent isothermal reaction for 24 min. The decrease of the CO formation rate in the isothermal region is caused by progressive methanol consumption and carbon poisoning of the catalyst surface. Experiments at 0.12 mbar/0.24 mbar methanol/water (i.e. the same partial pressures as used in the AP-XPS studies) reveal essentially the same trends (Supporting Information, Scheme S3). Complete reaction mass balance involving stoichiometric hydrogen formation was verified by mass spectrometry analysis.

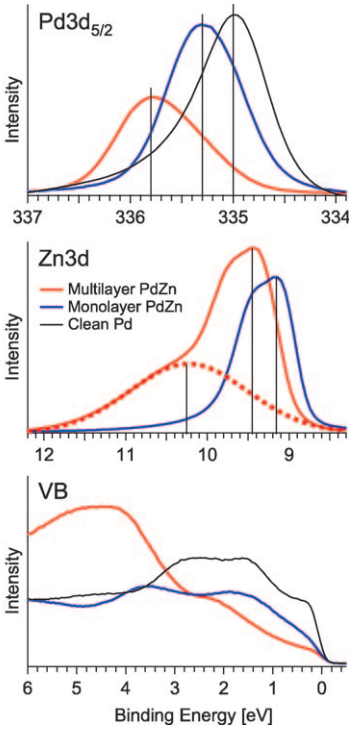

Figure 3. AP-XPS spectra (Pd 3d, Zn 3d, and valence-band (VB) regions) acquired in situ during MSR on the PdZn 1:1 multilayer (red curves) and monolayer alloy (blue curves). For comparison, the respective clean Pd spectra are added (black lines). The oxidized ZnOH component is highlighted by the dashed red line (middle panel). To obtain equal information depths for all spectra the Pd 3d spectra were recorded with 650 eV photon energy, the Zn 3d and valence-band regions at 120 eV. Reaction conditions: 0.12 mbar methanol, 0.24 mbar water, 553 K. All spectra show raw unsmoothed data.

with an increased density of states close to the Fermi level and upward shifted Pd 4d features. The result is a valence-band spectrum approaching that of clean Pd. The most important difference is evident from the Zn 3d spectra acquired under MSR reaction conditions (that is, in the presence of H_2O). Whereas the multilayer alloy activates water by forming a ZnOH species, resulting in the 10.25 eV shoulder in Figure 3 (dashed-red peak fit, middle panel), this species is not present on the monolayer alloy under identical conditions (Figure 3, blue curve). Consequently, the monolayer alloy does not activate water, and the CH_2O formed from methanol is not converted into CO_2, but rather dehydrogenated to CO.

The results from the Pd 3d and valence-band spectra were corroborated by the corresponding C 1s spectra (Supporting Information, Figure S4). Signatures of CH_2O or related oxygenates were observed up to 505 K for the multilayer alloy. Around 570 K and higher, the surface CH_2O was replaced by CO, indicating the transformation of multilayer to monolayer alloy. The O 1s data could not be reliably evaluated because of the strong overlap with the Pd 3p signal.

Our data provide clear evidence that both the geometric and the electronic structures of the multilayer and monolayer alloys are significantly different. The CO_2-selective multilayer alloy features a lowered density of states close to the Fermi edge and low-lying Pd 4d states. In addition it has surface ensembles of PdZn exhibiting a "Zn-up/Pd-down" corrugation, which are the "bifunctional" active sites both for efficient water activation and for steering the methanol dehydrogenation towards CH_2O.

The pronounced electronic and structural effects on the catalytic properties of the topmost active layer are driven by the composition of the second ("subsurface") and deeper layers, through variations of the Zn coordination of both the Pd and Zn surface atoms.

The interaction of different formaldehyde species in different adsorption geometries with either OH(ads) or O(ads) in different bonding geometries gives rise to several mechanistic scenarios for CO_2 formation. For example, dioxomethylene has been proposed as an intermediate.[12–14] However, in the absence of unambiguous spectroscopic information regarding further reaction intermediates, we can only speculate on possible adsorption geometries and reaction pathways (see Supporting Information, Scheme S5). Pinning down the detailed mechanism remains a challenging task for both theory and experiment.

In summary, we demonstrated that a model catalyst approach, combined with spectroscopic surface analysis under UHV and during reaction at realistic pressures, can be utilized to explain the different CO_2 selectivities of multilayer and monolayer PdZn surface alloys, despite their identical surface stoichiometry of 1:1. The subsurface layers steer the electronic and geometric structure of the topmost, catalytically active layer (valence-band density of states, corrugation) and are thus mainly responsible for the surface chemistry. The properties of the active sites are not sufficiently described by considering only the constituting atoms of the active ensemble but require the consideration of neighboring sites. This scenario limits the applicability of a "single site" concept, at least for systems with extended electronic structures.

Future studies will reveal whether this concept can be extended to oxide-supported PdZn nanoparticles.

Received: October 16, 2009
Revised: November 24, 2009
Published online: March 29, 2010

Keywords: heterogeneous catalysis · methanol steam reforming · PdZn alloy · surface chemistry · water activation

[1] a) A. Szizybalski, F. Girgsdies, A. Rabis, Y. Wang, M. Niederberger, T. Ressler, *J. Catal.* **2005**, *233*, 297; b) N. Iwasa, N. Takezawa, *Top. Catal.* **2006**, *22*, 215.
[2] S. Penner, B. Jenewein, H. Gabasch, B. Klötzer, D. Wang, A. Knop-Gericke, R. Schlögl, K. Hayek, *J. Catal.* **2006**, *241*, 14.
[3] A. Bayer, K. Flechtner, R. Denecke, H.-P. Steinrück, K. H. Neyman, N. Rösch, *Surf. Sci.* **2005**, *600*, 78.
[4] H. Gabasch, S. Penner, B. Jenewein, B. Klötzer, A. Knop-Gericke, R. Schlögl, K. Hayek, *J. Phys. Chem. B* **2006**, *110*, 11391.
[5] G. Weirum, M. Kratzer, H.-P. Koch, A. Tamtögl, J. Killmann, I. Bako, A. Winkler, S. Surnev, F. P. Netzer, R. Schennach, *J. Phys. Chem. C* **2009**, *113*, 9788.
[6] E. Jeroro, J. M. Vohs, *J. Am. Chem. Soc.* **2008**, *130*, 10199.
[7] W. Stadlmayr, S. Penner, B. Klötzer, N. Memmel, *Surf. Sci.* **2009**, *603*, 251.
[8] a) G. Rupprechter, H. Unterhalt, M. Morkel, P. Galletto, L. Hu, H.-J. Freund, *Surf. Sci.* **2002**, *502–503*, 109; b) G. Rupprechter, *Adv. Catal.* **2007**, *51*, 133.
[9] T. Conant, A. M. Karim, V. Lebarbier, Y. Wang, F. Girgsdies, R. Schlögl, A. Datye, *J. Catal.* **2008**, *257*, 64.
[10] K. Neyman, K. H. Lim, Z.-X. Chen, L. V. Moskaleva, A. Bayer, A. Reindl, D. Borgmann, R. Denecke, H.-P. Steinrück, N. Rösch, *Phys. Chem. Chem. Phys.* **2007**, *9*, 3470.
[11] I. Bakó, R. Schennach, G. Palinkas, *J. Phys. Conf. Ser.* **2008**, *100*, 052067.
[12] Z.-M. Hu, H. Nakatsuji, *Chem. Phys. Lett.* **1999**, *313*, 14.
[13] N. Takezawa, N. Iwasa, *Catal. Today* **1997**, *36*, 45.
[14] K. Takahashi, N. Takezawa, H. Kobayashi, *Appl. Catal.* **1982**, *2*, 363.

